

Relative amplitude of the variations of the total electron content according to the data of the GPS global network

N. P. Perevalova,¹ E. L. Afraimovich,¹ I. V. Zhivetiev,¹ and E. A. Kosogorov¹

Received 20 December 2005; revised 16 November 2006; accepted 20 February 2007; published 27 April 2007.

[1] A method is developed that makes it possible to estimate the relative amplitude dI/I of the variations of the total electron content (TEC) corresponding to the mean (MS) and intermediate (IS) scales of ionospheric irregularities (from 300 to 30 km). This method is based on the evaluation of TEC variations from the data of the global GPS network. The results of the analysis of the diurnal and latitudinal dependencies of dI/I and distribution probability $P(dI/I)$ for 52 days with different level of geomagnetic activity are presented. The statistical estimates were obtained from the analysis of 10^6 samples of 2-hour-long TEC series. To obtain statistically significant results, we have chosen three latitudinal zones provided on the Web by the maximum number of GPS sites: high-latitude zone of the Northern America (50–80°N, 200–300°E; 59 stations), midlatitude zone of the Northern America (20–50°N, 200–300°E; 817 stations), and the equatorial zone (20°S–20°N, 0–360°E; 76 stations). It was found that on the average the relative amplitude of the TEC variations varies within the range 0–10% proportionally to the value of the Kp geomagnetic index. This dependence is best pronounced at high latitudes (the proportionality coefficient $k = 0.37$), is weaker at middle latitudes ($k = 0.2$), and is the weakest at the equator ($k < 0.1$). In quiet conditions the nighttime dI/I values significantly exceed the daytime value by a factor of 3–5 at low and high latitudes and by a factor of 2 at middle latitudes. At a high level of magnetic field disturbances, the geomagnetic control of the amplitude of TEC variations at high and middle latitudes is much more significant than the regular diurnal variations. At the equator, on the average, the amplitude of both MS and IS variations in quiet and disturbed periods almost does not differ. At high latitudes one can note insignificant difference in the TEC variations amplitude both for MS and IS travelling ionospheric disturbances (TID) (by not more than a factor of 2). At middle latitudes the difference may reach an order of magnitude. This indicates that there is a cardinal depletion of the slope of the power spectrum of TEC disturbances because of a decrease of the amplitude of the small-scale parts of the spectrum. The amplitude of TEC variations almost does not depend on solar activity index $F_{10.7}$. The obtained results do not always agree with the known mechanisms of generation and propagation of ionospheric irregularities at various latitudes and may be useful for development of the theory. *INDEX TERMS*: 2439 Ionosphere: Ionospheric irregularities; 2427 Ionosphere: Ionosphere/atmosphere interactions; 6964 Radio Science: Radio wave propagation; *KEYWORDS*: transionospheric propagation; GPS system; ionospheric behavior.

Citation: Perevalova, N. P., E. L. Afraimovich, I. V. Zhivetiev, and E. A. Kosogorov (2007), Relative amplitude of the variations of the total electron content according to the data of the GPS global network, *Int. J. Geomagn. Aeron.*, 7, GI1007, doi:10.1029/2005GI000132.

1. Introduction

¹Institute of Solar-Terrestrial Physics, Irkutsk, Russia

[2] Study of ionospheric irregularities is one of the important problems of the geophysics and radiophysics. Ionospheric irregularities influence radio wave propagation within the broad radio wave range from hundreds of meters to tens

of centimeters used in radiocommunication, radiolocation, and radioastronomy [Afraimovich and Karachentsev, 2003; Afraimovich et al., 1992, 1994, 1999; Lawrence et al., 1964; Spoelstra and Kelder, 1984].

[3] The middle-scale (MS) irregularities with a typical period of 20–60 min are manifested in the form of middle-scale and large-scale (depending on the propagation velocity) travelling ionospheric disturbances (TID) and are an ionospheric response of acoustic gravity waves (AGW) [Afraimovich et al., 2000; Hines, 1960; Hocke and Schlegel, 1996; Hunsucker, 1982; Oliver et al., 1997]. TID produce refractive distortions of transionospheric radio signals [Afraimovich et al., 1992, 1994, 1999; Jacobson et al., 1995; Lawrence et al., 1964; Spoelstra and Kelder, 1984].

[4] Intermediate-scale irregularities (IS) with a period of 2–10 min and dimensions of 10–30 km are usually associated with the spread F [Bowman, 1990, 1991, 1992] and by size are close to small-scale irregularities causing scintillations of transionospheric signals [Yeh and Liu, 1982].

[5] The experimental study of the ionospheric irregularities is based on the use of radiophysical methods of ionospheric sounding. Recently, considerable progress has been achieved in the study of ionospheric irregularities using the new technology of radio sounding by signals of the satellite navigation system GPS [Davies and Hartmann, 1997]. This technology allows us to obtain data on variations of the total electron content (TEC) in the ionosphere with high spatial and time resolution in various regions of the globe. Advancements in the development of this technology enabled study of characteristics of wide range of the ionospheric irregularities as a function of local time, latitude, geomagnetic field disturbances, and other geophysical factors.

[6] The goal of this paper is a complex study of spatial and temporal characteristics of the absolute (dI) and relative (dI/I) amplitudes of TEC variations in quiet and disturbed geomagnetic conditions.

[7] Section 2 contains general information on the experiment. Section 3 is dedicated to the description of the method of data processing. The main results of the analysis of the diurnal dependence and statistical characteristics of the amplitude of TEC variations as a function of the Kp and $F_{10.7}$ indices are described in sections 4 and 5. The problem on the correspondence between TEC amplitude characteristics and parameters of local irregularities of the electron density is discussed in section 6. The obtained results are discussed in section 7.

2. General Information on the Experiment and Database

[8] To study the dependence of the absolute and relative amplitude of TEC variations on various geophysical factors for the period from 1999 to 2005, 12 quiet days ($Kp < 3$) and 40 disturbed days ($Kp > 3$) were chosen. The dates included in this study, the corresponding maximum and minimum values of Dst and Kp indices, and also the daily mean values of the solar activity index $F_{10.7}$ are given in Table 1. The

selected data cover mostly fall and spring equinox and a few winter days.

[9] To obtain statistically significant results, we (in some sense arbitrarily) chose three latitudinal zones with the maximum number of GPS stations presented in the Web. They are high-latitude zone of North America (50–80°N, 200–300°E; 59 stations), midlatitude zone of North America (20–50°N, 200–300°E; 817 stations), and equatorial zone (20°S–20°N, 0–360°E; 76 stations).

3. Method of Data Processing

[10] The standard GPS technology provides a means for calculation of slant TEC I_s along line of sight (LOS) between GPS satellite and receiver based on phase measurements at each of spaced two-frequency GPS receivers. Data of phase measurements are contained in the RINEX files, available at ftp://sopac.ucsd.edu/pub/.

[11] A method of the TEC calculating was specified and validated in a series of publications [e.g., Afraimovich, 2000]. We reproduce here only the final formula for phase measurements:

$$I_s = \frac{1}{40.308} \frac{f_1^2 f_2^2}{f_1^2 - f_2^2} [(L_1 \lambda_1 - L_2 \lambda_2) + \text{const} + nL] \quad (1)$$

where $L_1 \lambda_1$ and $L_2 \lambda_2$ are additional paths of the radio signal caused by the phase delay in the ionosphere [m]; L_1 and L_2 represent the number of phase rotations at the frequencies f_1 and f_2 ; λ_1 and λ_2 stand for the corresponding wavelengths [m]; const is the unknown initial phase ambiguity [m]; and nL are the errors in determining the phase path [m].

[12] Phase measurements in the GPS can be performed with a high degree of accuracy corresponding to the error of TEC determination of at least 10^{13} m^{-2} when averaged on a 30-s time interval, with some uncertainty of the initial value of TEC, however. Filtered out in the range of periods 30–60 min, the standard deviation of TEC series is not worse than $0.2 \times 10^{13} \text{ m}^{-2}$.

[13] To normalize the response amplitude, we have converted “slant” TEC I_s to an equivalent “vertical” value I [Klobuchar, 1986]:

$$I = I_s \cos \left[\arcsin \left(\frac{R_z}{R_z + h_{\max}} \cos \theta_s \right) \right] \quad (2)$$

where R_z is the Earth’s radius, $h_{\max} = 300 \text{ km}$ is the height of the F_2 -layer maximum, and θ_s is the elevations of the LOS.

[14] Then we selected continuous TEC series $I(t)$ with a duration of about 2 hours from the obtained TEC data so that we had 22 overlapping time intervals with a 1-hour shift for the day. We used specified threshold of 30° for elevations θ_s to the GPS satellites. $I(t)$ series for all GPS sites in the region under consideration and for all visible satellites were filtered in the timescale of 20–60 min and 2–10 min using running average filtering. Standard deviation σ of TEC variations was calculated for each series. The σ values were averaged on all series; thus we got for each 2

Table 1. Statistics of the Experiment

| Year | Day of Year | Date | <i>Dst</i> min/max | <i>Kp</i> min/max | $F_{10.7}$ | Number of TEC Series |
|------|----------------|--------|-----------------------|----------------------|------------|-------------------------|
| 1999 | 283 | 10 Oct | -84/18 | 2.7/5.7 | 160.3 | 18,600 |
| 2000 | 097 | 6 Apr | -287/ - 6 | 1.7/8.3 | 179.4 | 2936 |
| | 098 | 7 Apr | -288/ - 92 | 3.7/8.7 | 175.8 | 2833 |
| | 190 | 8 Jul | 2/14 | 0.3/2.3 | 216.2 | 20,252 |
| | 196 | 14 Jul | -21/26 | 3/6 | 212.1 | 4323 |
| | 197 | 15 Jul | -300/10 | 4/9 | 219.9 | 3336 |
| | 198 | 16 Jul | -295/ - 111 | 3/8 | 227.6 | 4450 |
| 2001 | 090 | 31 Mar | -358/30 | 6/9 | 247.9 | 4504 |
| | 091 | 1 Apr | -215/ - 63 | 3/6 | 248.6 | 4650 |
| | 092 | 2 Apr | -90/ - 24 | 3/4 | 342.5 | 18,172 |
| | 093 | 3 Apr | -30/ - 6 | 1/3 | 218.4 | 22,182 |
| | 094 | 4 Apr | -17/26 | 2/5 | 205.6 | 16,360 |
| | 103 | 13 Apr | -66/ - 12 | 1/7.3 | 138.2 | 21,714 |
| | 104 | 14 Apr | -58/ - 15 | 2/4.3 | 138.8 | 20,916 |
| | 275 | 2 Apr | -88/ - 54 | 4/5 | 202.6 | 5002 |
| | 276 | 3 Oct | -179/ - 29 | 3/7 | 192.6 | 5133 |
| | 277 | 4 Oct | -101/ - 47 | 1.7/4.3 | 186.2 | 5669 |
| | 278 | 5 Oct | -43/ - 2 | 1/3 | 179 | 17,581 |
| | 279 | 6 Oct | -19/ - 8 | 0.3/3 | 176.1 | 23,110 |
| | 291 | 18 Oct | -1/13 | 0/1.7 | 224.06 | 21,389 |
| 2002 | 092 | 2 Apr | -41/ - 5 | 1.3/4.3 | 206.4 | 16,292 |
| 2003 | 301 | 28 Oct | -48/ - 17 | 3/4 | 284.4 | 19,843 |
| | 302 | 29 Oct | -345/ - 41 | 3/9 | 291 | 18,368 |
| | 303 | 30 Oct | -401/ - 108 | 5/9 | 264 | 19,551 |
| | 304 | 31 Oct | -320/ - 72 | 4/8.3 | 245.4 | 18,890 |
| | 305 | 1 Nov | -31/14 | 2.7/5 | 217.7 | 18,094 |
| | 306 | 2 Nov | 0/24 | 3/4 | 256.7 | 17,530 |
| | 307 | 3 Nov | 0/38 | 2/3 | 163.9 | 21,321 |
| | 308 | 4 Nov | -48/51 | 2/7 | 303.6 | 21,180 |
| | 324 | 20 Nov | -429/30 | 1/9 | 168.1 | 17,538 |
| | 325 | 21 Nov | -320/ - 75 | 2/6.7 | 173.3 | 19,446 |
| | 353 | 19 Dec | -7/6 | 0/0.7 | 120.6 | 26,432 |
| | 354 | 20 Dec | -31/31 | 0.3/4.7 | 125.7 | 29,344 |
| | 355 | 21 Dec | -38/ - 10 | 3/4.3 | 128.5 | 17,424 |
| | 356 | 22 Dec | -28/ - 12 | 3/3.7 | 131.7 | 29,755 |
| 2004 | 311 | 6 Nov | -5/2 | 0/0.7 | 125.3 | 28,590 |
| | 312 | 7 Nov | -128/51 | 0.7/8 | 135.1 | 28,912 |
| | 313 | 8 Nov | -373/ - 120 | 2.7/8.7 | 122 | 25,995 |
| | 314 | 9 Nov | -223/ - 90 | 5/8.7 | 196.4 | 22,526 |
| | 315 | 10 Nov | -289/ - 119 | 4.3/8.7 | 103.5 | 26,750 |
| | 316 | 11 Nov | -115/ - 53 | 2.3/5 | 93.5 | 25,291 |
| | 317 | 12 Nov | -109/ - 45 | 3.3/4.7 | 94.7 | 26,079 |
| | 318 | 13 Nov | -75/ - 54 | 0.7/2.3 | 95 | 27,182 |
| | 360 | 25 Dec | -32/ - 8 | 1.3/4 | 90.06 | 25,418 |
| | 361 | 26 Dec | -27/ - 13 | 1.7/3 | 89.06 | 25,253 |
| | 362 | 27 Dec | -33/ - 6 | 1/2.7 | 93.5 | 28,638 |
| 2005 | 017 | 17 Jan | -81/ - 19 | 4/6.3 | 133.8 | 23,509 |
| | 018 | 18 Jan | -125/ - 41 | 5/7.7 | 125.6 | 22,157 |
| | 019 | 19 Jan | -96/ - 62 | 2.3/6.7 | 128.8 | 21,456 |
| | 020 | 20 Jan | -65/ - 41 | 2/4.7 | 118.8 | 23,986 |
| | 087 | 28 Mar | -11/1 | 0.3/1.7 | 78.4 | 25,242 |
| SUM | | | | | | 961,104 |

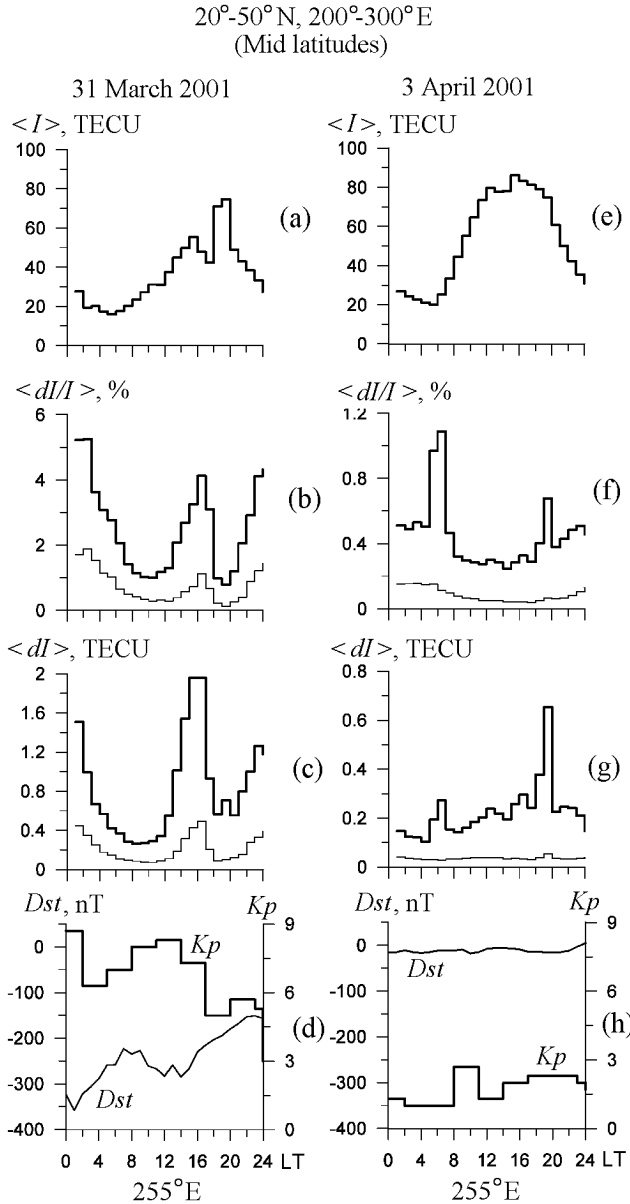


Figure 1. (d, h) Indices of geomagnetic activity Dst and Kp ; diurnal dependencies of (a, e) the averaged values of TEC $\langle I \rangle$, (b, f) of relative $\langle dI/I \rangle$, and (c, g) of absolute $\langle dI \rangle$ amplitude MS (thick lines) and IS (thin lines) TEC variations during the magnetic storm on 31 March 2001 and quiet day on 3 April 2001. Middle latitudes.

hours time interval the mean absolute values $dI = [\sum \sigma_i]/m$, where $i = 1, 2, \dots, m$; m is a total number of series. The dI represents an absolute value of the amplitude of TEC variations. The distribution of the number of series I_m over days is shown in Table 1. The total number of analyzing series is about 10^6 .

[15] The relative amplitude dI/I_0 is determined by normalization of the dI to the background I_0 value, where I_0 is the absolute vertical TEC obtained with 2-hour time resolu-

tion from the global TEC maps in the IONEX format (the so-called global ionospheric maps (GIM) [Mannucci *et al.*, 1998]). The spatial range of GIM is 0–360° in longitude and 90°S–90°N in latitude. The spatial resolution is restricted by the dimensions of an elementary GIM cell (5° and 2.5° in longitude and latitude, respectively). For the normalization, the I_0 values are used for the GIM cell closest to the GPS station used for determination of the dI value.

[16] The series I_m , dI_m , and dI/I_m were averaged over the chosen area to obtain the mean values of TEC $\langle I \rangle$, of the absolute amplitude $\langle dI \rangle$ and of the relative amplitude $\langle dI/I \rangle$ of TEC variations in the period ranges of MS and IS ionospheric irregularities.

4. Diurnal Dependence of the Amplitude of TEC Variations

[17] Now we consider in detail the diurnal dependencies of the averaged values of TEC $\langle I \rangle$, of the relative $\langle dI/I \rangle$ and of the absolute $\langle dI \rangle$ amplitudes of TEC variations for several quiet and disturbed days. We start our analysis with the conditions of the midlatitude ionosphere and then will note the features of the high-latitude and equatorial ionosphere.

[18] To illustrate a typical diurnal dependence at middle latitudes, we chose four days: moderately disturbed (quiet) days on 3 April 2001 and 3 November 2003 and also the days when strong magnetic storms were observed: 31 March 2001 and 30 October 2003 (Figures 1 and 2, right and left, respectively). The geomagnetic activity indices Dst and Kp are shown in Figures 1d, 2d, 1h, and 2h, respectively. The diurnal dependencies of the averaged TEC values $\langle I \rangle$ are shown in Figures 1a, 2a, 1e, and 2e. The dependencies of the relative $\langle dI/I \rangle$ amplitude of the TEC variations are shown in Figures 1b, 2b, 1f, and 2f. The same values for the absolute $\langle dI \rangle$ amplitude of the TEC variations are shown in Figures 1c, 2c, 1g, and 2g. MS and IS ionospheric irregularities are shown by thick and thin lines, respectively.

[19] Figures 1 and 2 show a smooth variation of $\langle I \rangle$ in quiet period with the TEC maximum reaching in the daytime (1200–1600 LT). This behavior corresponds to the regular TEC behavior obtained for a quiet period by the measurement of the turning angle of the polarization plane of the VHF signals of geostationary satellites [Afraimovich *et al.*, 1999; Davies, 1980] and also by the measurement of the difference in the phase and group delay of the GPS signals at two coherently related frequencies [Kotake *et al.*, 2006; Mannucci *et al.*, 1998]. The absolute amplitude $\langle dI \rangle$ for MS and IS ionospheric irregularities varies within 0.1–0.7 TECU (TECU = 10^{16} m⁻²) and 0.01–0.03 TECU, respectively, reaching maximum value also in the daytime.

[20] However, in disturbed conditions the character of $\langle dI \rangle$ dependence changes considerably. The value of the absolute amplitude $\langle dI \rangle$ increases by a factor of 3–4 (Figure 1) or even by an order of magnitude (Figure 2), reaching 3 TECU. At the same time the $\langle dI \rangle$ maximum shifts to the time moment corresponding to the maximum deviation of the Dst and very high level $Kp = 9$. This effect is especially visual

during the main phase of the strong magnetic storm on 30 October 2003. Nevertheless, the maximum values of $\langle dI \rangle$ are observed mainly in the daytime.

[21] The diurnal behavior of the relative amplitude $\langle dI/I \rangle$ differs cardinally from the corresponding dependence of $\langle dI \rangle$. It is especially distinctly pronounced in quiet conditions: the $\langle dI/I \rangle$ maximums for MS and IS ionospheric irregularities are observed at night, not in the daytime.

[22] In disturbed conditions the changes in $\langle dI/I \rangle$ are governed not only by diurnal behavior but by the magnetic field as well. The vertical line in Figure 2 shows the moment of a sharp peak of $\langle dI \rangle$ on 30 October 2003, when the value of $\langle dI \rangle$ reached 3 TECU. This example shows that the geomagnetic control of the amplitude of TEC variations at high levels of the magnetic field disturbances appear to be more important than the regular diurnal variations.

[23] At high latitudes (Figures 3 and 4) the diurnal dependence of TEC and its variations in quiet and disturbed conditions differ from the same at middle latitudes. First, both have higher amplitudes. For example, the absolute and relative amplitudes $\langle dI \rangle$ and $\langle dI/I \rangle$ during the main phase of the magnetic storm on 30 October 2003 reach 16 TECU and 50%, respectively.

[24] Moreover, at high latitudes one can note a slight difference in amplitudes $\langle dI \rangle$ and $\langle dI/I \rangle$ of TEC variations for ionospheric irregularities of different scales (not more than by a factor of 2). At middle latitudes this difference reaches an order of magnitude. This fact indicates that there is a cardinal decrease in the declination of the power spectrum of TEC disturbances due to the increase in the amplitude of the small-scale part of the spectrum [Afraimovich *et al.*, 2001].

[25] Even more distinction with middle latitudes is observed at the equator (Figures 5 and 6). First, in disturbed conditions the increase in the relative and absolute amplitudes as compared to quiet conditions is weaker (not more than by a factor of 1.5–2). The maximum value of the relative amplitude $\langle dI/I \rangle$ systematically is observed at night. This regularity is not broken even during the main phase of the magnetic storm independent of the local time during which this phase occurs. This conclusion agrees completely with the widely known morphology of ionospheric scintillations at equatorial latitudes based on numerous measurements by different ionospheric sounding methods [Aarons, 1982; Yeh and Liu, 1982].

[26] For the quiet days the above noted latitudinal dependencies are pronounced especially clearly at daily mean values. Figure 7 shows the diurnal dependencies of the averaged values of the absolute $\langle dI \rangle$ (Figures 7a–7c) and relative $\langle dI/I \rangle$ (Figures 7d–7f) amplitudes of IS (thin lines) and MS (thick lines) TEC variations for 12 quiet days ($Kp < 3$): Figures 7a and 7d, 7b and 7e, and 7c and 7f correspond to high, middle, and equatorial latitudes, respectively. One can see from Figure 7 that the maximum values of the relative amplitude of the TEC variations almost do not depend on latitude and are observed mainly at night.

[27] In quiet conditions the nighttime dI/I values significantly exceed the daytime value by a factor of 3–5 at low and high latitudes and by a factor of 2 at middle latitudes. At a high level of magnetic field disturbance, the geomag-

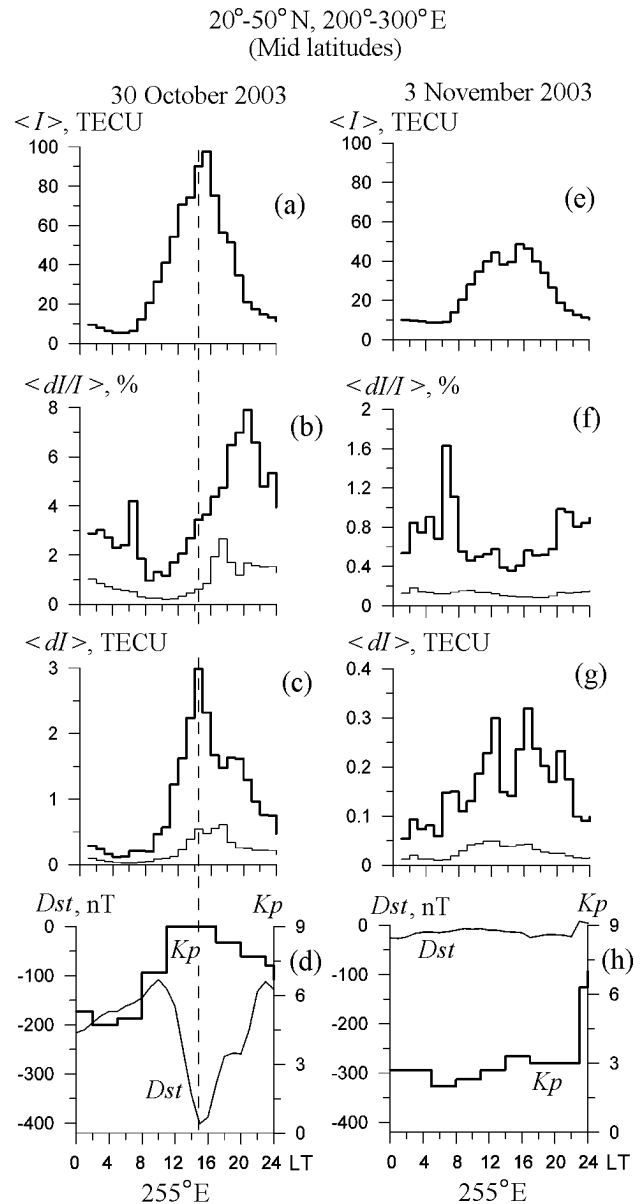


Figure 2. (d, h) Indices of geomagnetic activity Dst and Kp ; diurnal dependencies of the averaged values (a, e) of TEC $\langle I \rangle$, (b, f) of relative $\langle dI/I \rangle$, and (c, g) of absolute $\langle dI \rangle$ amplitude MS (thick lines) and IS (thin lines) TEC variations during the magnetic storm on 30 October 2003 and moderately disturbed quiet day on 3 November 2003. Middle latitudes. The vertical line shows the moment of sharp peak of the absolute amplitude of TEC variations.

netic control of the TEC variation amplitude is even more significant than the regular diurnal variations.

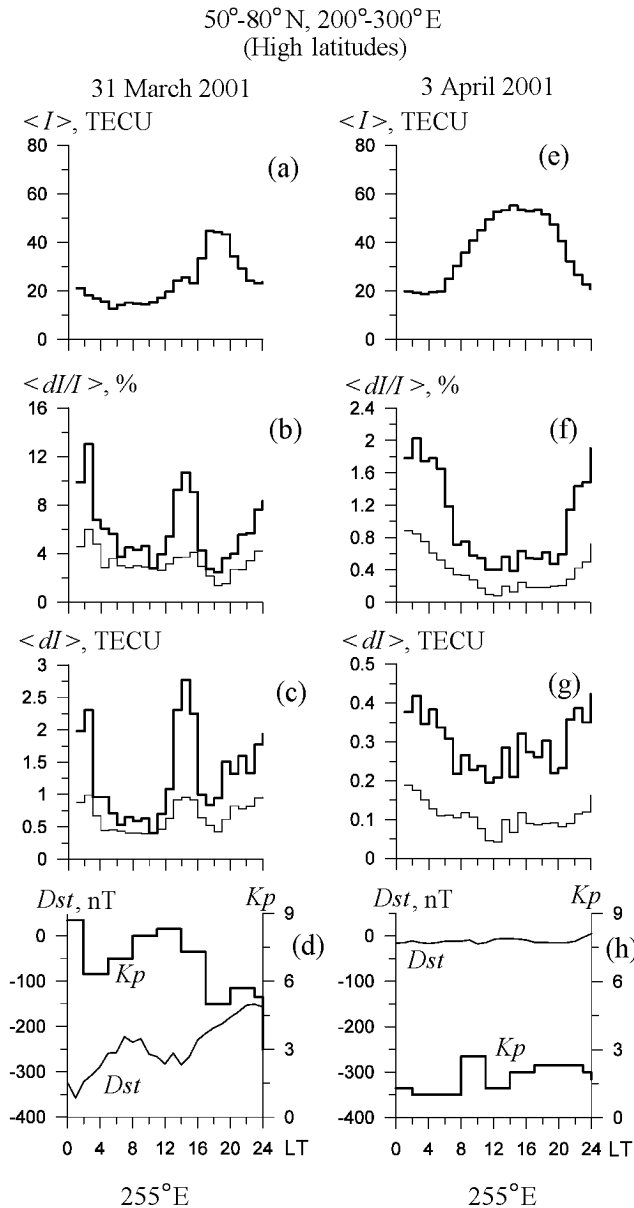


Figure 3. Same as in Figure 1, but for high latitudes.

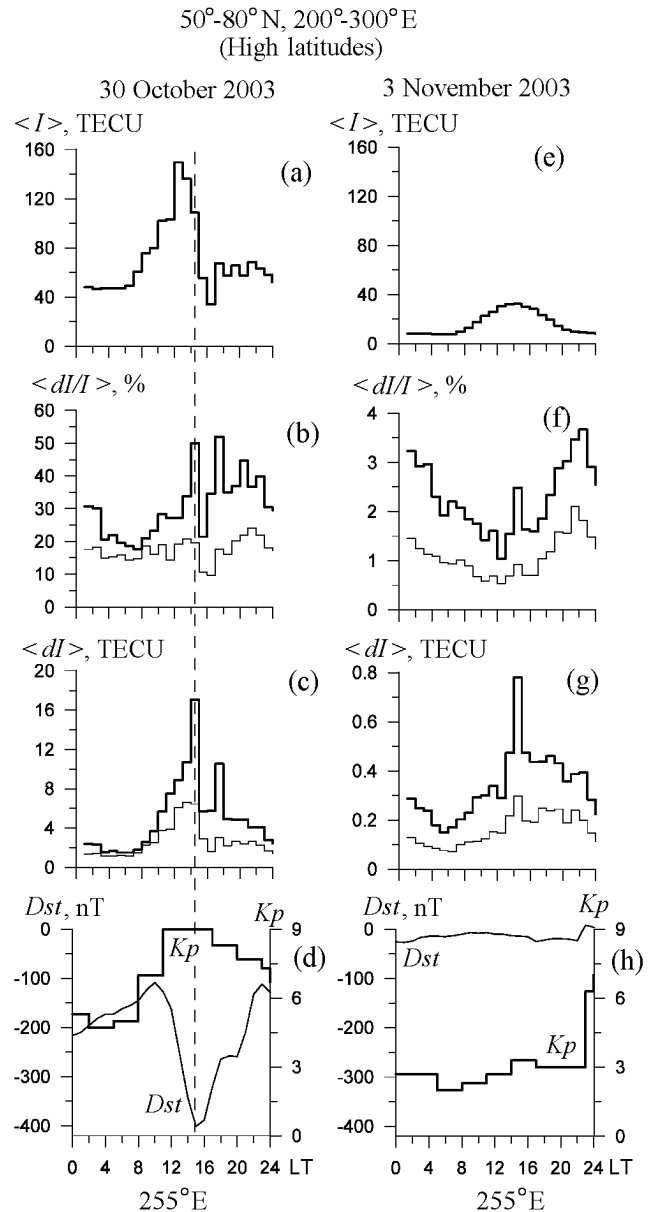


Figure 4. Same as in Figure 2, but for high latitudes.

5. Distribution of the Probability of the Relative Amplitude of TEC variations and Dependence on the Kp and $F_{10.7}$

[28] Statistical characteristics of the relative amplitude of TEC variations: first, probability distributions $P(\langle dI/I \rangle)$ are required to study mechanisms of generation of ionospheric irregularities and to evaluate transionospheric radio signal distortions.

[29] Figure 8 shows the normalized distributions $P(\langle dI/I \rangle)$ of the relative amplitude TEC variations in quiet (thin line, index 1) and disturbed (thick line, index 2) conditions. MS and IS ionospheric irregularities are shown on the left and

on the right in Figure 8: Figures 8a and 8d, 8b and 8e, and 8c and 8f correspond to high and middle latitudes and to the equatorial zone, respectively. The total amounts of 2-hour averaged series over the entire area of the North America were 288 and 936 for quiet and disturbed periods, respectively. The approximation of the total normalized distributions $P(\langle dI/I \rangle)$ for the same conditions is shown in Figure 9. The most probable values of $\langle dI/I \rangle$ in quiet (X_1) and disturbed (X_2) conditions are shown.

[30] One can see from Figures 8 and 9 that at high latitudes in quiet periods the relative amplitude of MS disturbances does not exceed 4–5%, whereas in disturbed periods it may reach 10–12%. Similar dependence is also observed for IS variations of TEC with the only difference that the

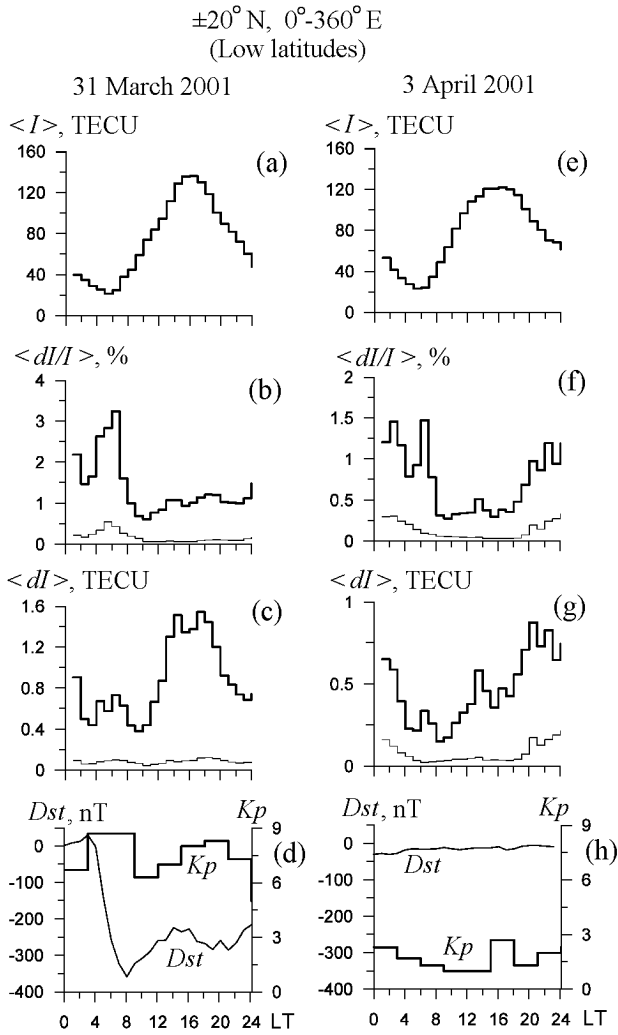


Figure 5. Same as in Figure 1, but for the equatorial zone.

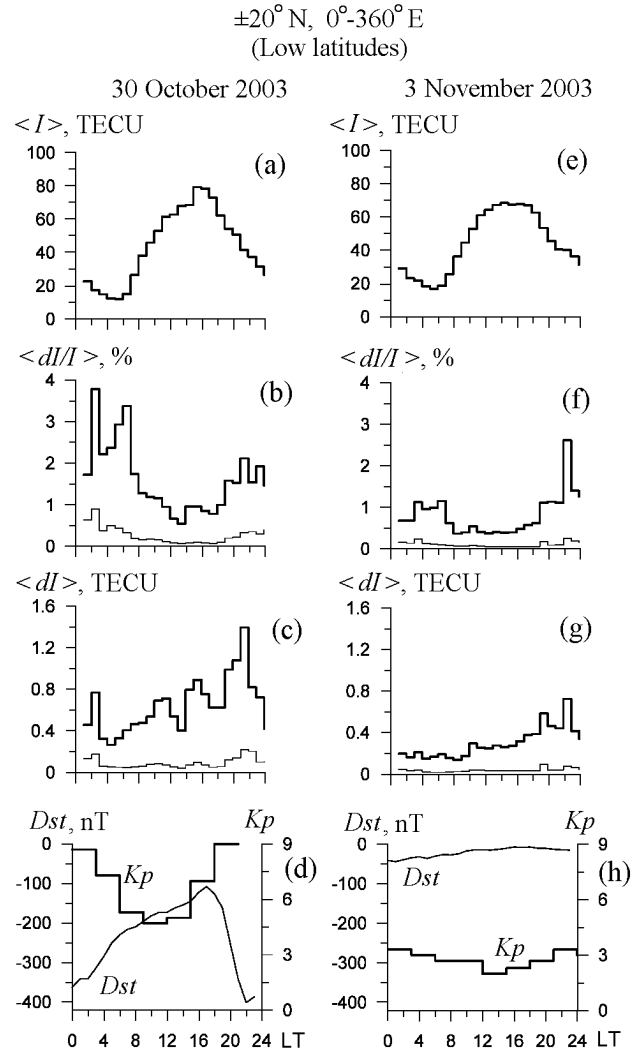


Figure 6. Same as in Figure 2, but for the equatorial zone.

general disturbance level is by a factor of 4–5 less than for MS.

[31] At middle latitudes, $\langle dI/I \rangle$ dependence on the geomagnetic disturbance level is similar to that at high latitudes. However, on the whole, the amplitude of the MS and IS disturbances decreases by a factor of 2–3 and 5, respectively. At the equator, on the average, the amplitudes of MS and IS variations in quiet and disturbed periods almost do not differ.

[32] The difference in the dependence of the TEC relative amplitude on the geomagnetic disturbance level at various latitudes in the best way is illustrated in the regression dependencies of the amplitude of TEC variations on the values of the Kp index shown in Figure 10. Points show the values of $\langle dI/I \rangle$ averaged over 3-hour-long intervals, and the thick line shows the approximating lines: MS TID are given in Figures 10a–10c, IS TID in Figures 10d–10f; Figures 10a

and 10d, 10b and 10e, and 10c and 10f correspond to high, middle, and equatorial latitudes, respectively.

[33] On the average, the relative amplitude of TEC variations is proportional to the value of the geomagnetic Kp index. This dependence is most pronounced at high latitudes (the proportionality coefficient $k = 0.37$), it is weaker at middle latitudes ($k = 0.2$) and weakest at the equator ($k < 0.1$).

[34] The regression dependencies of the amplitude of TEC variations on the $F_{10.7}$ are presented in Figure 11. Points show the values of $\langle dI/I \rangle$ averaged over 3-hour-long intervals. The thick line is an approximating line: MS TID are given in Figures 11a–11c and IS TID are given in Figures 11d–11f; Figures 11a and 11d, 11b and 11e, and 11c and 11f correspond to high, middle, and equatorial latitudes, respectively. One can see that the amplitude of TEC variations almost does not depend on solar activity.

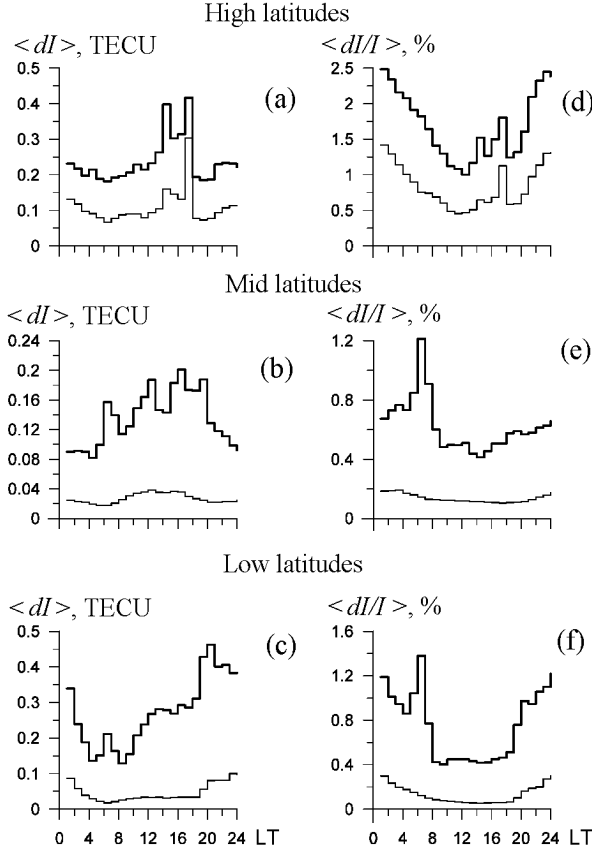


Figure 7. Total diurnal dependencies of the averaged values of (left) the absolute $\langle dI \rangle$ and (right) relative $\langle dI/I \rangle$ amplitudes of MS (thick lines) and IS (thin lines) TEC variations for 12 quiet days ($Kp < 3$); (a and d) high latitudes; (b and e) middle latitudes; and (c and f) equatorial latitudes.

6. Correspondence Between the Amplitude Characteristics of TEC Variations and Parameters of Local Irregularities of Electron Density

[35] The estimate of the relative amplitude dN/N of a local disturbance of the electron density is very important for physics of ionospheric irregularities (and also for calculation of statistical characteristics of transionospheric signals). The transition from the amplitude characteristics of TEC variations to values of dN/N is far from being simple.

[36] First, the amplitude of TEC disturbance dI demonstrates a strong aspect dependence because of the integral character of transionospheric sounding. The maximum amplitude dI corresponds to wave disturbances with the wave vector \mathbf{K} perpendicular to the direction \mathbf{r} of the LOS [Afraimovich *et al.*, 1992], i.e., when the condition is fulfilled,

$$\tan \theta = -\frac{\cos(\alpha_s - \alpha)}{\tan \theta_s} \quad (3)$$

where α and θ are the azimuth and the elevation angle of

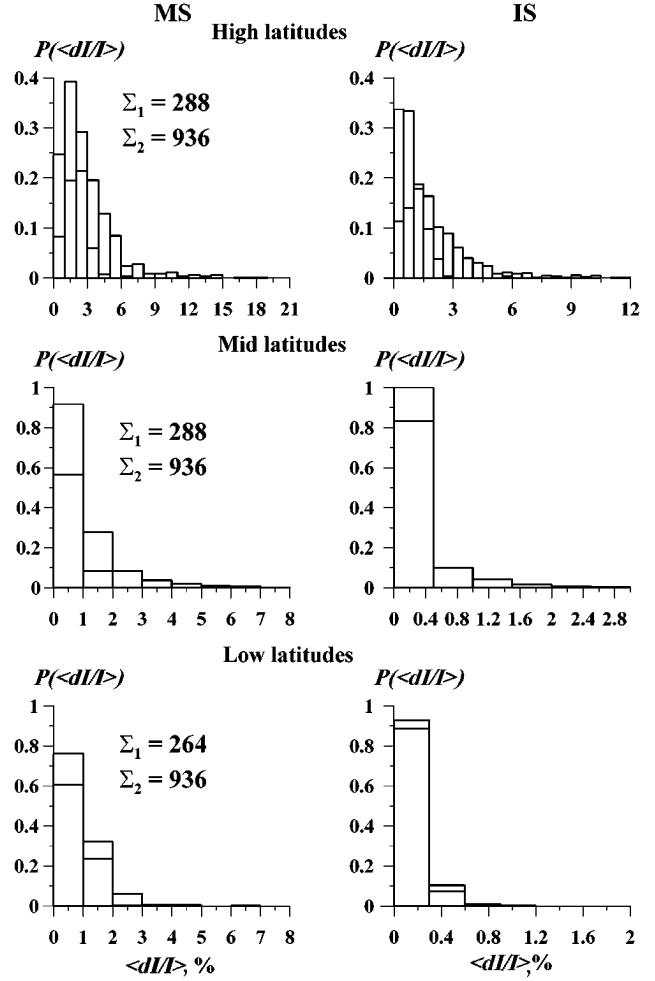


Figure 8. Total normalized distribution $P(\langle dI/I \rangle)$ of the relative amplitude of TEC variations for quiet (thin line) and disturbed (thick line) conditions: (left) MS and (right) IS; (a and d) high latitudes, (b and e) middle latitudes, and (c and f) equatorial latitudes.

the wave vector \mathbf{K} of TID, and α_s and θ_s are the azimuth and the elevation angle of LOS.

[37] Aspect dependence of the amplitude of TEC disturbance is important in studying wave disturbances. Condition (3) limits the number of LOS for which reliable detecting of ionospheric irregularities on the background of noises is possible.

[38] *Afraimovich et al.*, [1992] have shown that for the Gaussian distribution of the electron density, the amplitude of TEC disturbance $M(\gamma)$ is determined by the aspect angle γ between the \mathbf{K} and \mathbf{r} vectors and also by the ratio of the disturbance wavelength λ to the half thickness of the ionization maximum Δ :

$$M(\gamma) \propto \exp\left(-\frac{\pi^2 \Delta^2 \cos^2 \gamma}{\lambda^2 \cos^2 \theta_s}\right) \quad (4)$$

For the phase velocity of about 200 m s^{-1} and the period of about 1000 s, the wavelength λ is comparable to the value

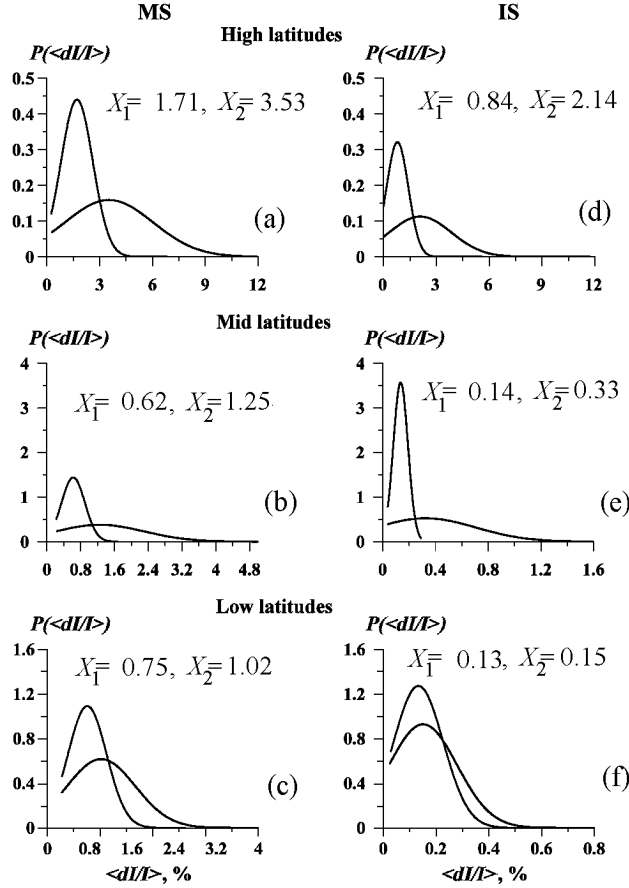


Figure 9. Approximation of the total normalized distributions $P(\langle dI/I \rangle)$ of the relative amplitude of TEC variations for quiet (thin line) and disturbed (thick line) conditions: (left) MS and (right) IS; (a and d) high latitudes, (b and e) middle latitudes, and (c and f) equatorial latitudes. $\Sigma_1 = 288, \Sigma_2 = 936$

of the half thickness Δ of the ionization maximum. At the values of the elevation angle θ_s equal to 30° , 45° , and 60° , the width of “the directivity diagram” $M(\gamma)$ at the level of 0.5 is equal to 25° , 22° , and 15° , respectively. If Δ exceeds the wavelength λ by a factor of 2, the directivity diagram becomes narrower in width by 14° , 10° , and 8° , respectively.

[39] The presence of magnetic field alters the picture of the motion transfer from the neutral gas to the electron component of the ionosphere. Since the magnetic field is not pulled by the neutral gas, the field lines may be considered as still. In this case, the approximation in which the motion of the electron component occurs only along the field lines with the velocity $u \cos \psi$, where ψ is the angle between the vector of the magnetic field and the vector \mathbf{u} of the neutral gas velocity, may be acceptable. Thus the amplitude of a disturbance of the electron density dN/N depends on the angular relations γ and ψ between three vectors.

[40] However, in our case, because of averaging of the results over directions to different satellites and also because of large number of GPS stations over a vast territory where

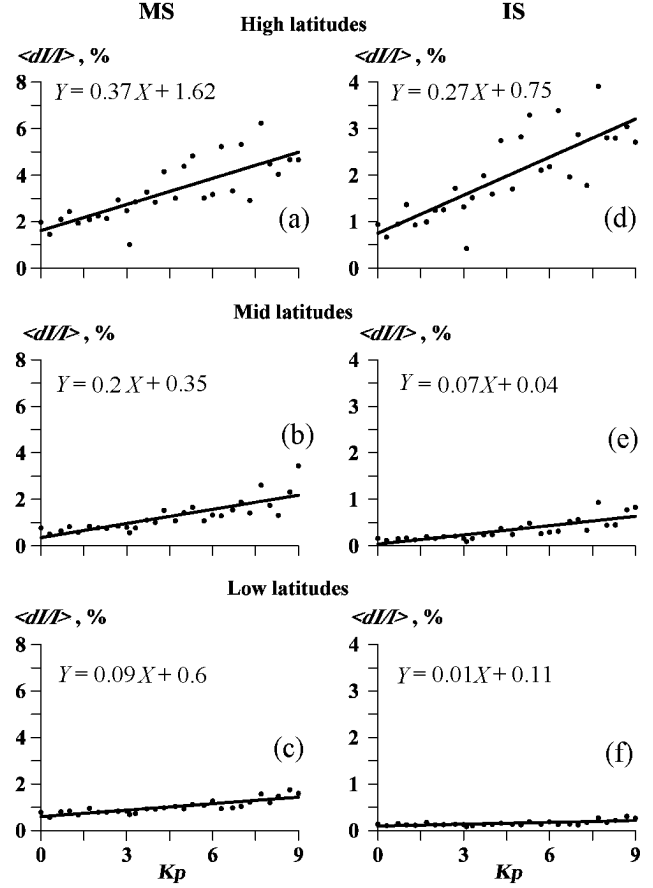


Figure 10. Regression dependencies of the amplitude of TEC variations on Kp index. Points show the averaged over 3-hour interval values of $\langle dI/I \rangle$; thick lines show approximating lines. (left) MS and (right) IS; (a and d) high latitudes, (b and e) middle latitudes, and (c and f) equatorial latitudes.

the values of γ and ψ angles vary within a wide range, aspect effects are pronounced not so strongly as for some variations in TEC.

[41] Thus the relation between dN/N and dI/I may be presented in the form

$$(dI/I) / (dN/N) = k_{\max} \quad (5)$$

where k_{\max} is the maximum value of the transitional coefficient from dN/N to dI/I under optimum aspect conditions.

[42] We performed a modelling to evaluate the value of k_{\max} . The model of TEC measurements developed by *Afraimovich and Peravalova* [2004] makes it possible to calculate spatial and time distribution of the local electron density N in the ionosphere along the LOS and then using the coordinates of the receiver and satellites to perform integrating N along the LOS with the given time step. As a result, time series of TEC similar to the input experimental data are obtained.

[43] The model of N takes into account vertical profile,

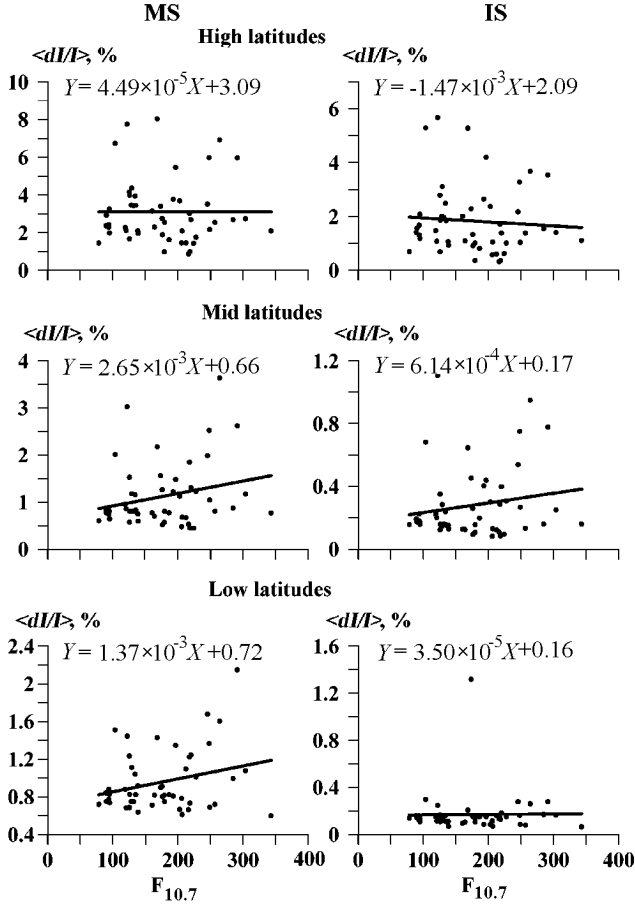


Figure 11. Regression dependencies of the amplitude of TEC variations on $F_{10.7}$ index. Points show the averaged over 3-hour interval values of $\langle dI/I \rangle$; thick lines show approximating lines. (left) MS and (right) IS; (a and d) high latitudes, (b and e) middle latitudes, and (c and f) equatorial latitudes.

diurnal and seasonal variations of the electron density governed by the solar zenith angle, and also irregular disturbance of N of smaller amplitude and spatial scales in the form of a superposition of propagating wave or isolated irregularities. The GPS satellite motion can be modelled by a few ways. A detailed description of the model was given by *Afraimovich and Perevalova* [2004].

[44] In this paper, diurnal and seasonal variations of N were neglected in the model calculations. A stationary isolated irregularity in the form of a sphere with radius R_d was chosen as a disturbance. The electron density within the irregularity smoothly decreases from the center to the periphery:

$$N_d = A_d \times \exp \left[\frac{(x - x_{\max})^2 + (y - y_{\max})^2 + (z - z_{\max})^2}{R_d} \right] \quad (6)$$

where A_d is the amplitude of the disturbance in the percent of the value N_{\max} within the maximum of the F_2 layer

(i.e., $A_d = dN/N$); x, y, z are the coordinates of the current point in the topocentric coordinates system (TCS) connected to the GPS receiver; $x_{\max}, y_{\max}, z_{\max}$ are the TCS coordinates of the irregularity center (point M). It was taken that the irregularity is located at a height of the F_2 layer maximum ($z_{\max} = 300$ km). The position of the irregularity relative to the GPS receiver (i.e., the coordinate center of TCS) was governed by the elevation angle θ and azimuth α of the radius vector of point M. Two cases were considered: $\theta = 45^\circ$ and $\theta = 60^\circ$. In both cases, $\alpha = 45^\circ$. The radius R_d of the irregularity consequently was chosen to be equal 30, 100, and 300 km. That corresponded to the irregularities scales considered in the paper. The relative amplitude of the disturbance dN/N in all cases was assumed to be equal to 10%.

[45] The visual motion of the GPS satellite within the interval from 1200 to 1300 UT was given by the change in the azimuth $\alpha_S(t)$ of LOS from 0 to 90° . The elevation angle $\theta_S(t)$ remained constant. The calculations were performed for two trajectories: $\theta_S = 45^\circ$ and $\theta_S = 60^\circ$. The trajectories were chosen in such a way that at one of them the LOS during the studied interval crossed the center of the electron density irregularity.

[46] The modelling results are shown in Figure 12. Figures 12a and 12e show the behavior of $\alpha_S(t)$. Figures 12b–12d and 12f–12h show the results of the calculations of TEC at $\theta_S = 45^\circ$ and $\theta_S = 60^\circ$, respectively. The I_{45} and I_{60} TEC dependencies for the trajectories with $\theta_S = 45^\circ$ and $\theta_S = 60^\circ$ are shown by thick and thin curves. LOS corresponding to I_{45} intersects the N irregularity center at the moment when $\alpha_S = 45^\circ$ (on the left). LOS corresponding to I_{60} intersects the irregularity center at the moment $\alpha_S = 45^\circ$ (on the right).

[47] In the cases when LOS does not cross the irregularity N (thin line in Figure 12b and thick line in Figure 12f), TEC remains constant during the entire observational time. It should have been expected at the constant elevation angle θ_S and the absence of the diurnal variations of N . A well-pronounced disturbance in the form of a single pulse in the TEC variations is well seen for the trajectories where LOS passes through the irregularity N . The width of the pulse is proportional to the irregularity radius R_d . The TEC maximum in the pulse is observed in the moment when the angle between LOS and radius vector of the center of the irregularity is minimal. It corresponds to $\alpha_S = \alpha = 45^\circ$. This moment is shown in the Figure 12 by the dashed line.

[48] The absolute amplitude of a TEC disturbance dI depends on several factors. First, it is proportional to R_d , because the length of LOS interval laying within disturbed values of N at other equal conditions increases with an increase of the irregularity scale. Moreover, dI depends on the mutual position of the irregularity N and LOS. One can clearly see in Figures 12c, 12d, 12g, and 12h that the highest values of dI are reached when LOS passes through the irregularity center. Both the disturbance amplitude dI and TEC value I are also determined by the elevation angle of LOS and the amplitude of the disturbance N in the irregularity.

[49] The calculated values of the relative amplitude dI/I of TEC disturbance and of the coefficient k_{\max} are shown in Table 2. Both parameters, as well as the values of dI and I ,

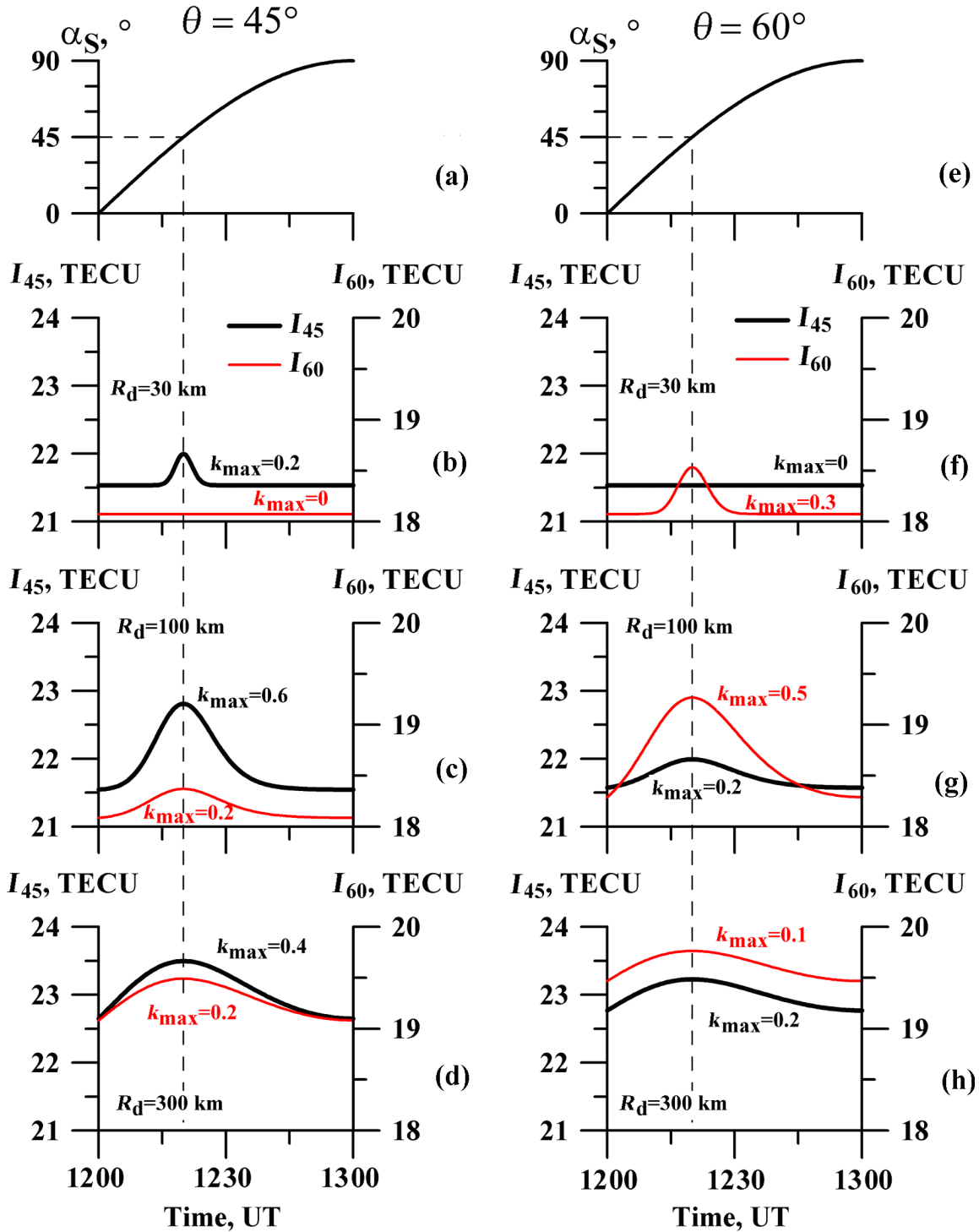


Figure 12. Modelling results. (a and e) Behavior of α_S . The results of the TEC calculations at (b–d) $\theta = 45^\circ$ and (f–h) $\theta = 60^\circ$. I_{45} and I_{60} are TEC dependencies for the trajectories with $\theta_S = 45^\circ$ and $\theta_S = 60^\circ$.

demonstrate considerable variability depending on the disturbance parameters, electron density, and measurements conditions.

[50] In the majority of cases, the value of k_{max} varies within 0–0.3. In the most favorable conditions of the reg-

istration, when LOS crosses the center of the N spherical irregularity, $k_{max} = 0.5 - 0.6$ (results 2 and 11 in Table 2). In this case the radius of the irregularity $R_d = 100$ km is comparable to the half thickness of the F2 layer. The latter means that the TEC disturbance with the relative amplitude

Table 2. Modelling Results

| Result | R_d , km | θ , deg | θ_S , deg | dI , TECU | I , TECU | dI/I , % | k |
|--------|------------|----------------|------------------|-------------|------------|------------|------|
| 1 | 30 | 45 | 45 | 0.499 | 21.5 | 2.3 | 0.2 |
| 2 | 100 | 45 | 45 | 1.210 | 21.6 | 5.6 | 0.6 |
| 3 | 300 | 45 | 45 | 0.796 | 22.7 | 3.5 | 0.4 |
| 4 | 30 | 45 | 60 | 0 | 18.074 | 0 | 0 |
| 5 | 100 | 45 | 60 | 0.271 | 18.1 | 1.5 | 0.2 |
| 6 | 300 | 45 | 60 | 0.391 | 19.1 | 2.1 | 0.2 |
| 7 | 30 | 60 | 45 | 0.036 | 21.5 | 0.2 | 0.02 |
| 8 | 100 | 60 | 45 | 0.391 | 21.6 | 1.8 | 0.2 |
| 9 | 300 | 60 | 45 | 0.428 | 22.8 | 1.9 | 0.2 |
| 10 | 30 | 60 | 60 | 0.460 | 18.074 | 2.6 | 0.3 |
| 11 | 100 | 60 | 60 | 0.967 | 18.3 | 5.3 | 0.5 |
| 12 | 300 | 60 | 60 | 0.264 | 19.5 | 1.4 | 0.1 |

$dI/I = 5\%$ can be caused by an electron density irregularity localized in the maximum of the $F2$ layer and having the relative amplitude dN/N not less than 10% and characteristic scale comparable to the half thickness of the $F2$ layer.

7. Discussion

[51] Our data agree with the results of measurements of the absolute amplitude $\langle dI \rangle$ of TEC variations obtained at transionospheric UHF sounding by signals of geostationary satellite ETS 2 [Afraimovich *et al.*, 1999] and also with the data of the analysis of the variation of TEC spectra according to the GPS data [Afraimovich and Karachentsev, 2003; Afraimovich *et al.*, 2001].

[52] Unexpectedly, the inverse dependence of the relative amplitude of the TEC variations in quiet period was found: the maximum values of $\langle dI/I \rangle$ are observed at night but not in the daytime. The latter means that the mechanisms of generation and propagation of AGW differ significantly in the daytime and at night. This is in agreement with conclusions of other researchers, for instance, based on the data of TEC measurements in Los Alamos (35.9°N, 106.3°W). Jacobson *et al.* [1995] claimed that the seasonal variations in MS TID occurrence rate and propagation directions are different in the daytime and at night. They showed that the daytime MS TID are formed mainly during the winter solstice and propagate southward, whereas the nighttime MS TID occur mainly during the summer solstice till the fall equinox and propagate northwestward.

[53] Kelley and Miller [1997] noted that the difference between the direction of MS TID propagation in the daytime and at night is responsible for the difference in MS TID generation. The amplitude of gravity waves grows at a depletion of the neutral density [Hines, 1960]. Larger amplitude of gravity waves is able to generate larger disturbances in plasma density, i.e., in the MS TID activity. On the other hand, the rate of the linear growth of a Perkins instability is also inversely proportional to the neutral density [Perkins, 1973]. Most probably the Perkins instability is a source of

nighttime MS TID though the rate of the linear growth is very small.

[54] Kotake *et al.* [2006] have found that MS TIDs activity during daytime is different from that during nighttime with respect to seasonal, solar activity, longitudinal, and latitudinal dependencies. Daytime MS TIDs activity is high in winter. On the other hand, seasonal variation of nighttime MS TIDs activity is coupled with its longitudinal variation. In the Japanese and Australian longitudinal sector, nighttime MS TIDs are most active near the June solstice, whereas in the European longitudinal sector it is most active near the December solstice. Nighttime MS TIDs activity at the Japanese and Australian longitudinal sector shows negative correlation with solar activity, whereas solar activity dependence is not seen in daytime MS TIDs activity. These results suggest that mechanisms causing MS TIDs could be different between daytime and nighttime.

[55] Hernandez-Pajares *et al.* [2006] have shown that the MS TIDs, which occur at daytime in local winter and nighttime in local summer, are related to the solar terminator and are modulated by the solar cycle.

[56] Then our conclusion regarding the difference mechanisms of generation and propagation of AGW in the daytime and at night agrees with data obtained by the Kelley and Miller [1997], Kotake *et al.* [2006], and Hernandez-Pajares *et al.* [2006].

[57] The delay by 2 hours of the sharp peak of $\langle dI/I \rangle$ relative quick variations in the magnetic field during the 30 October 2003 storm can be explained in the following way. Under the averaging, the main weight brings the midlatitude zone of GPS stations. This zone is located at a distance of about 2000 km from the southern boundary of the auroral source of TID that occurred during geomagnetic disturbances. The TID generated at the appearance of this source moves equatorward with velocity of about 300–400 m s⁻¹ [Afraimovich *et al.*, 2001; Hunsucker, 1982]. However, there is a large evidence of other mechanisms besides TID which could have the same observational features. For instance, Foster and Rideout [2005] have shown that for the same storm discussed in our paper (30 October 2003), TEC increase is observed at postnoon local times and related to subauroral electric fields.

8. Conclusions

[58] We have developed the method of estimation of relative amplitude dI/I of TEC variations from the GPS data and also the results of the analysis of the dI/I dependence on local time and latitude.

[59] We have found that on average, the relative amplitude of the TEC variations varies within the range from 0% to 10% proportional to the value of the geomagnetic index Kp . This dependence is most pronounced at high latitudes (the proportionality coefficient $k = 0.37$), is weaker at middle latitudes ($k = 0.2$), and is the weakest at the equator ($k < 0.1$). In quiet conditions the nighttime dI/I values significantly exceed the daytime ones (by a factor of 3–5 at low and high latitudes and by a factor of 2 at middle latitudes). At high levels of the magnetic field disturbance, the geomagnetic control of the amplitude of TEC variations is more important than regular diurnal variations.

[60] At high latitudes one can note insignificant difference of the amplitude of TEC variations for MS and IS ionospheric irregularities (not more than by a factor of 2; while at middle latitudes this factor reaches 10). This manifests a cardinal decrease of the power spectrum of TEC disturbances due to increase of the small-scale part of the spectrum.

[61] The analysis of the corresponding amplitude characteristics of TEC variations and parameters of local irregularities of the electron density showed that recalculation of these characteristics is possible only in the scope of some model of irregularity. In any case the relative amplitude of local electron density disturbances is higher than the amplitude of TEC variations.

[62] The obtained results are not always in accordance with the known mechanisms of generation and propagation of ionospheric irregularity at various latitudes and can be useful for development of the theory.

[63] **Acknowledgments.** The authors thank V. A. Medvedev for his interest to the work and fruitful discussion and also S. V. Voykov for his help in the preliminary treating of the data. The work was supported by the Russian Foundation for Basic Research (project 05-05-64634), integration grant SB RAS–FEB RAS 3.24. We thank the staff of the Scripps Orbit and Permanent Array Center (SOPAC) for presentation of the used in the paper initial data of the global network of ground-based two-frequency GPS receivers.

References

- Aarons, J. (1982), Global morphology of ionospheric scintillations, *Proc. IEEE*, *70*(4), 360.
- Afraimovich, E. L. (2000), GPS global detection of the ionospheric response to solar flares, *Radio Sci.*, *35*(6), 1417, doi:10.1029/2000RS002340.
- Afraimovich, E. L., and V. A. Karachentsev (2003), Testing of the transionospheric radiochannel using data from the global GPS network, *Ann. Geophys.*, *46*(6), 1229.
- Afraimovich, E. L., and N. P. Perevalova (2004), Modeling of total electron content measurements from the GPS radiointerferometer, in *Sol. Terr. Phys.*, *4* (in Russian), p. 71, Inst. of Sol. Terr. Phys. Russ. Acad. of Sci., Irkutsk.
- Afraimovich, E. L., A. I. Terechov, M. Yu. Udodov, and S. V. Fridman (1992), Refraction distortions of transionospheric radio signals caused by changes in a regular ionosphere and by travelling ionospheric disturbances, *J. Atmos. Terr. Phys.*, *54*(7/8), 1013, doi:10.1016/0021-9169(92)90068-V.
- Afraimovich, E. L., S. V. Fridman, and N. P. Minko (1994), Spectral and dispersion characteristics of medium-scale travelling ionospheric disturbances as deduced from transionospheric sounding data, *J. Atmos. Sol. Terr. Phys.*, *56*(11), 1431, doi:10.1016/0021-9169(94)90109-0.
- Afraimovich, E. L., O. N. Boitman, E. I. Zhovty, A. D. Kalikhman, and T. G. Pirog (1999), Dynamics and anisotropy of traveling ionospheric disturbances as deduced from transionospheric sounding data, *Radio Sci.*, *34*(2), 477, doi:10.1029/1998RS900004.
- Afraimovich, E. L., E. A. Kosogorov, L. A. Leonovich, K. S. Palamarchouk, N. P. Perevalova, and T. G. Pirog (2000), Determining parameters of large-scale travelling ionospheric disturbances of auroral origin using GPS-arrays, *J. Atmos. Sol. Terr. Phys.*, *62*(7), 553, doi:10.1016/S1364-6826(00)00011-0.
- Afraimovich, E. L., E. A. Kosogorov, O. S. Lesyuta, A. F. Yakovets, and I. I. Ushakov (2001), Geomagnetic control of the spectrum of travelling ionospheric disturbances based on data from a global GPS network, *Ann. Geophys.*, *19*(7), 723.
- Bowman, G. G. (1990), A review of some recent work on midlatitude spread F occurrence as detected by ionosondes, *J. Geomagn. Geoelectr.*, *42*, 109.
- Bowman, G. G. (1991), Nighttime mid-Latitude travelling ionospheric disturbances associated with mild spread F conditions, *J. Geomagn. Geoelectr.*, *43*(8), 899.
- Bowman, G. G. (1992), Upper atmosphere neutral-particle density variations compared with spread-F occurrence rates at locations around the world, *Ann. Geophys.*, *10*, 676.
- Davies, K. (1980), Recent progress in satellite radio beacon studies with particular emphasis on the ATS 6 radio beacon experiment, *Space Sci. Rev.*, *25*(4), 357, doi:10.1007/BF00241558.
- Davies, K., and G. K. Hartmann (1997), Studying the ionosphere with the Global Positioning System, *Radio Sci.*, *32*(4), 1695, doi:10.1029/97RS00451.
- Foster, J. C., and W. Rideout (2005), Midlatitude TEC enhancements during the October 2003 superstorm, *Geophys. Res. Lett.*, *32*, L12S04, doi:10.1029/2004GL021719.
- Hernandez-Pajares, M., J. M. Juan, and J. Sanz (2006), Medium-scale traveling ionospheric disturbances affecting GPS measurements: Spatial and temporal analysis, *J. Geophys. Res.*, *111*, A07S11, doi:10.1029/2005JA011474.
- Hines, C. O. (1960), Internal atmospheric gravity waves at ionospheric heights, *Can. J. Phys.*, *38*, 1441.
- Hocke, K., and K. Schlegel (1996), A review of atmospheric gravity waves and travelling ionospheric disturbances: 1982–1995, *Ann. Geophys.*, *14*, 917.
- Hunsucker, R. (1982), Atmospheric gravity waves generated in the high-latitude ionosphere: A review, *Rev. Geophys. Space Phys.*, *20*, 293.
- Jacobson, A. R., R. C. Carlos, R. S. Massey, and G. Wu (1995), Observations of travelling ionospheric disturbances with a satellite beacon radio interferometer: Seasonal and local time behavior, *J. Geophys. Res.*, *100*, 1653, doi:10.1029/94JA02663.
- Kelley, M. C., and C. A. Miller (1997), Electrodynamics of midlatitude spread F : 3. Electrohydrodynamic waves? A new look at the role of electric fields in thermospheric wave dynamics, *J. Geophys. Res.*, *102*, 11,539, doi:10.1029/96JA03841.
- Klobuchar, J. A. (1986), Ionospheric time-delay algorithm for single-frequency GPS users, *IEEE Trans. Aerosp. Electron. Syst.*, *23*(3), 325, doi:10.1109/TAES.1987.310829.
- Kotake, N., Y. Otsuka, T. Tsugawa, T. Ogawa, and A. Saito (2006), Climatological study of GPS total elec-

- tron content variations caused by medium-scale travelling ionospheric disturbances, *J. Geophys. Res.*, *111*, A04306, doi:10.1029/2005JA011418.
- Lawrence, R. S., C. G. Little, and J. A. Chivers (1964), The influence of the ionosphere upon radio wave propagation "Earth-space", *Proc. IEEE*, *52*(4), 5.
- Mannucci, A. J., B. D. Wilson, D. N. Yuan, C. M. Ho, U. J. Lindqwister, and T. F. Runge (1998), A global mapping technique for GPS-derived ionospheric TEC measurements, *Radio Sci.*, *33*, 565, doi:10.1029/97RS02707.
- Oliver, W. L., Y. Otsuka, M. Sato, T. Takami, and S. Fukao (1997), Climatology of *F* region gravity waves propagation over the middle and upper atmosphere radar, *J. Geophys. Res.*, *102*, 14,449, doi:10.1029/97JA00491.
- Perkins, F. (1973), Spread *F* and ionospheric currents, *J. Geophys. Res.*, *78*, 218.
- Spoelstra, T. A., and H. Kelder (1984), Effects produced by the ionosphere on radio interferometry, *Radio Sci.*, *19*, 779.
- Yeh, K. C., and C. H. Liu (1982), Radio wave scintillations in the ionosphere, *Proc. IEEE*, *70*(4), 324.
-
- E. L. Afraimovich, E. A. Kosogorov, N. P. Perevalova and I. V. Zhivetiev, Institute of Solar-Terrestrial Physics, 126 Lermontov str., Irkutsk 664033, Russia. (afra@iszf.irk.ru)